Characterization of the Mechanical Properties of Sensitive Clay by Means of Indentation Tests

Vincenzo Silvestri[1(✉)] and Claudette Tabib[2]

[1] École Polytechnique, Montreal, Canada
vincenzo.silvestri@polymtl.ca
[2] Montreal, Canada

Abstract. Instrumented indentation tests were carried out on specimens of undisturbed clay, using various indenters at a constant rate of penetration of 0.5 mm/min. These tests were performed with 20-mm in diameter conical indenters with apical angles of 60°, 80°, 97°, and 144.3°, as well as with a Vickers indenter of semi-apical angle of 68.7°. Such tests allowed the determination of both the undrained shear strength and the deformation modulus of the clay. The undrained shear strength was found by assuming that a fully plastic stress field resulted from indenter penetration and by using slip-line theory. The deformation modulus was computed by assuming that the clay behaved elastically during initial penetration. The theory proposed by Love (1939) and later extended by Sneddon (1948, 1965) was used to obtain values of Young's modulus. The expanding cavity model or ECM proposed by Johnson (1970, 1985) was also employed for the interpretation of test results obtained with both sharp and blunt indenters.

One of the most significant findings of the present study is that the structure of the undisturbed clay suffers severe and progressive breakdown with increasing penetration during indentation, which results in a dramatic decrease of the strength and deformation parameters of the clay. Comparison between the undrained shear strength deduced from the quasi-static indentation tests and the dynamic Swedish fall-cone tests, also indicates that S_u obtained from the latter tests are much higher than the corresponding data derived from the indentation tests. It is believed that the possible cause of the overestimation of the undrained shear strength deduced from the Swedish fall-cone tests is related to the very high strain rate experienced by the falling cone.

The paper also presents a brief review of the most pertinent theories that are used for the interpretation of indentation tests.

Keywords: Indentation tests · Conical and pyramidal indenters · Sensitive clay · Young's modulus · Undrained shear strength · Comparisons

1 Introduction

Different test methods are available for the determination of the mechanical properties of materials. The results of these methods are employed for the design of engineering structures and as a basis for comparison and selection of materials. For instance, uniaxial tension and compression tests are commonly used to determine mechanical

L. Hoyos and H. Shehata (Eds.): GeoMEast 2019, SUCI, pp. 1–18, 2020.
https://doi.org/10.1007/978-3-030-34206-7_1

properties of metals and alloys, like Young's modulus, yield strength, and strain-hardening characteristics. In geotechnical engineering, triaxial tests, unconfined compression tests, simple shear tests, and Swedish fall-cone tests fulfill a similar role in the determination of the short-term strength parameters of clays.

As an alternative and appropriate method to determine the mechanical properties of materials, indentation tests have been proposed by many researchers (Tabor 1951; Johnson 1970, 1985; Oliver and Pharr 1992; Fischer-Cripps 2002, 2007). The main advantages of indentation tests are the following: (a) They do not require a large quantity of material: a well-polished and flat surface is sufficient to generate a large set of data; and (b) The measurement is non-destructive in nature as the impression is generally confined to a small region of the sample. According to the load-penetration data recorded during indentation, the mechanical properties of the specimen including Young's modulus E, yield strength σ_y, hardness H, and viscoelastic deformation parameters may be determined (Tabor 1951; Johnson 1985; Oliver and Pharr 1992; Fischer-Cripps 2007). The International Organization for Standardization (ISO) and the American Society for Testing and Materials (ASTM) issued standards which cover depth-sensing indentation testing for determining hardness and other material parameters (ISO 2002, 2007; ASTM 2003, 2007).

It is generally agreed that hardness is a measure of a material's resistance to permanent penetration by another harder material (Fischer-Cripps 2002). Of particular interest in indentation testing is the area of the contact zone found from the dimensions of the contact perimeter. The mean contact pressure p_m, as given by the indenter load P divided by the area of contact A, is a useful normalizing parameter; it has the additional advantage of having actual physical meaning (Fischer-Cripps 2002). The value of the mean contact pressure at which there is no additional increase in load is related to the hardness (Tabor 1951). In addition, the mean contact pressure is taken equal to the hardness H for indentation test methods that employ the projected area of contact A_p at this limiting condition.

Theoretical analyses of indentation problems have received attention from a number of investigators, since Prandtl (1920) developed a slip line solution for a two-dimensional punch on a semi-infinite plastic medium. A detailed analysis of wedge indentation was given by Hill et al. (1947) and Hill (1950), and Shield (1955) obtained a similar solution for axisymmetric indentation by a flat circular punch. These solutions apply to rigid plastic materials and are based on the slip line theory. Later, Lockett (1963) performed a numerical analysis of conical indentation based on the slip line theory and obtained solutions for apical angles $2\alpha \geq 105^{o}$. Lockett's solution was extended to other conical indenters by Houlsby and Wroth (1982) and Chitkara and Butt (1992).

Another line of approach to understanding indentation is semi-empirical in nature. Tabor (1951) presented a correlation between the mean contact pressure p_m and the yield stress σ_y. The correlation is expressed as:

$$p_m = H = C\,\sigma_y \tag{1}$$

where C is a constraint factor, the value of which depends on the type of specimen and the geometry of the indenter. For example, C = 3 for materials with a large ratio E/σ_y

(i.e., metals) and C = 1 to 1.5 for low values of E/σ_y (i.e., glasses and ceramics). To describe the correlation in Eq. 1, Johnson (1970) adopted the model of Marsh (1964) who, following Bishop et al. (1945) and Samuels and Mulhearn (1957), considered the plastic deformed zone beneath a blunt indenter as the expansion of a spherical cavity in an elastic-plastic solid under an internal hydrostatic pressure. Johnson (1970) included the effect of the indenter geometry.

In spite of these analyses, detailed solutions of indentation problems for realistic stress-strain relationships and indenter shapes are still lacking because of the very complex stress and strain fields produced by indentations. To resolve some of the uncertainties, indentation problems have been also approached using the finite element method of analysis in which indentations are simulated by means of rigid or elastic indenters on elastic, elastic-plastic, and viscoelastic materials (Barquins and Maugis 1982; Bhattacharya and Nix 1988; Giannakopoulos et al. 1994; Cheng and Li 2000; Riccardi and Montanari 2004; Guha et al. 2014; Hu et al. 2015).

While a large number of analytic and numerical studies on indentation have been conducted, commensurate experimental investigations, whose primary aim is to understand the elastic-plastic flow field beneath the indenter, are less common. Keeping this in view, an experimental study was undertaken on the influence of the cone indenter apical angle on the determination of the shear strength and Young's modulus of undisturbed overconsolidated sensitive clay of eastern Canada. Conical indenters with apical angles of 60^o, 80^o, 97^o, and 144.3^o, as well as a Vickers indenter (a square pyramid with opposite faces at an angle of 134.6^o and edges at 147^o) were used in the test program.

The present paper is organized in the following manner. In the next section, pertinent experiments, theoretical analyses, and simulations that have been conducted previously are reviewed with the objective of putting the current work in proper perspective. Thereafter, the section on the test program describes the clay and the experiments conducted in this study, whereas the section on the analysis presents results, discussions, and comparisons. The paper closes with conclusions and some brief remarks about future directions in research in this area.

2 Background

2.1 Conventional Analysis of Indentation Tests

In a typical indentation test, load P and depth of penetration h are recorded as load is applied from zero to some maximum load P_{max} and then from maximum load back to zero. If plastic deformation occurs, then there is a residual impression left in the surface of the specimen. When load is removed from the indenter, the material attempts to regain its original shape, but is prevented from doing so because of plastic deformation. However, there is some degree of recovery due to the relaxation of the elastic strains within the material (Fischer-Cripps 2002). The form of the compliance curves, that is, load versus depth of penetration curves, for the most common types of indenter (i.e., spherical, pyramidal, and conical) are very similar and a typical curve is shown in Fig. 1. In this figure (see also Fig. 2), h_r is the depth of the residual impression, h_{max} is

the depth from the original surface at maximum load, h_e is the elastic recovery during unloading, h_a is the distance from the edge of the circle of contact, as shown in Fig. 2, $h_p = h_{max} - h_a$, and dP/dh which is the slope of the initial portion of the unloading curve gives an estimate of the elastic modulus of the material.

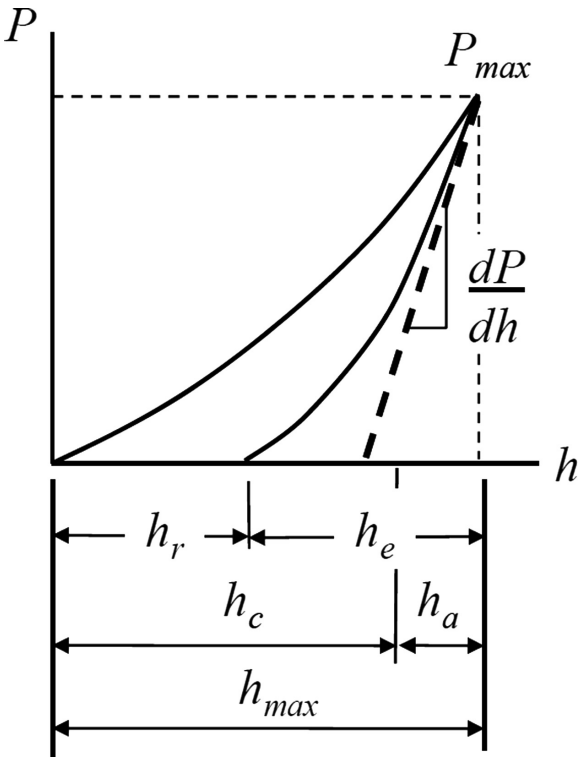

Fig. 1. Typical compliance curve from indentation test (after Fischer-Cripps 2007)

Indentation testing in many materials results in both elastic and plastic deformation of the indented specimen. In brittle materials, plastic deformation most commonly occurs with sharp indenters such as conical and pyramidal indenters. In ductile materials, plasticity may be readily induced with a blunt indenter such as a sphere or cylindrical flat-headed punch. Indentation tests are routinely used in the measurement of hardness, but conical and pyramidal indenters may be used to investigate other mechanical properties such as strength, toughness, and internal residual stresses (Yu and Blanchard 1996; Zeng and Chiu 2001; Fischer-Cripps 2002). Indentation tests involving spherical or conical indenters, first used as the basis for theories of hardness, enabled various criteria to be established. The most well-known criterion is that of Hertz, who postulated that an absolute value of hardness was the least value of pressure beneath a spherical indenter necessary to produce a permanent deformation at the center of the area of contact.

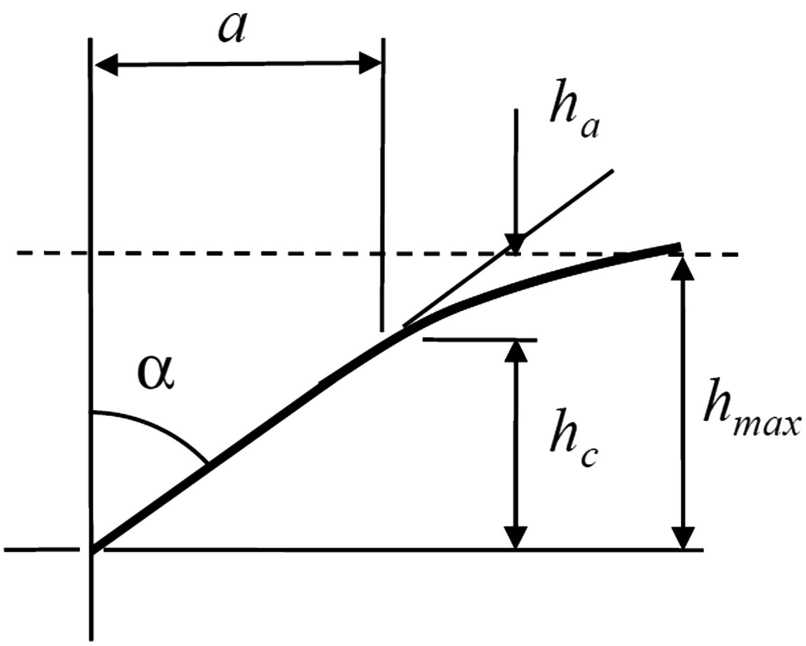

Fig. 2. Geometry of conical indentation (after Fischer-Cripps 2007)

The mean contact pressure, and, hence, the indentation hardness, for an impression made with a spherical indenter is given by:

$$p_m = H = 4P/\pi d^2 = P/\pi a^2 \tag{2}$$

where a is the radius and d is the diameter of the contact circle (the latter is assumed to be equal to the diameter of the residual impression left in the surface of the specimen upon removal of the load). The mean contact pressure determined in this way is often called the Meyer hardness. Meyer (1908) found that there was an empirical relationship between the diameter of the residual impression and the applied load, and this is known as Meyer's law:

$$P = k\,d^n \tag{3}$$

where k and n are constants for the specimen material. It has been shown that the value of n is insensitive to the radius of the spherical indenter and is related to the strain-hardening exponent x of the material according to (Fischer-Cripps 2002):

$$n = x + 2 \tag{4}$$

Values of n were found to range between 2 and 2.5, the higher value applying to annealed materials, while the lower value applying to work-hardened materials (i.e., low values of x). The strain-hardening exponent x plays an important role in the

constitutive relationships of elastic-plastic materials, as the mechanical properties of specimens can be approximated by a uniaxial stress-strain response given by:

$$\sigma = E \in,\ \sigma \leq \sigma_y/E \tag{5a}$$

and

$$\sigma = b \in^x,\ \sigma \geq \sigma_y/E \tag{5b}$$

where σ is the applied stress, $\in$ is the resulting strain, and b is defined as

$$b = \sigma_y\left(E/\sigma_y\right)^x \tag{6}$$

The material is elastic-plastic for x = 0.

Remark 1
For x = 0 and n = 2, Eq. 3 which reduces to $P = k\ d^2$ is often called Fick's law. In addition, for a conical indenter of apical angle 2α, substitution of the radius of contact a for the depth of penetration h_p (Fig. 2) results in $P = k\ h^2 \tan^2\alpha$ for Fick's law or more generally, $P = k^* h^2$, where $k^* = k \tan^2\alpha$.

Remark 2
Indenters can be classified into two categories- sharp or blunt. The criteria upon which a particular indenter is classified, however, are subjective. For example, some authors classify sharp indenters as those resulting in permanent deformation in the specimen upon removal of the load. However, others prefer to classify a conical or pyramidal indenter having an equivalent cone semi-apical angle $\alpha \geq 70^o$ as being blunt. For these, the response of the material follows that predicted by the expanding cavity model proposed by Johnson (1970) or the elastic constraint model of Tabor (1951), depending on the type of specimen material and magnitude of the load. For sharp indenters, it is generally observed that plastic flow occurs according to the slip line theory and the specimen behaves as a rigid plastic material.

2.2 Elastic Approach

The classical approach to finding the stresses and displacements in an elastic half-space produced by surface tractions is due to Boussinesq (1985) and Cerruti (1882) who made use of the theory of potential. Partial results based upon such theory were obtained by Love (1939) for the case of an elastic half-space indented by a rigid cone. Because Boussinesq's method does not lend itself to practical analysis, Sneddon (1948) used the integral transform technique to obtain the same result and to evaluate all the components of stress within the solid. In addition, Sneddon (1965) derived a relationship between the load P and the depth of penetration h in the axisymmetric

Boussinesq problem for a rigid punch of arbitrary shape. For a conical indenter of apical angle 2α, Sneddon's relationship reduces to (see also Fig. 2):

$$P = \pi a^2 E \cot\alpha/2\left(1 - \nu^2\right) \tag{7}$$

where E and ν are respectively Young's modulus and Poisson's ratio of the specimen material, and a is the radius of the circle of contact. The depth profile of the deformed surface within the area of contact is

$$h(r) = (\pi/2 - r/a)\, a \cot\alpha \tag{8}$$

At the circle of contact, the quantity a cot α represents the depth of penetration h_p. Substitution of Eq. 8 for r = 0 in Eq. 7 yields

$$P = 2 E h^2 \tan\alpha/\pi\left(1 - \nu^2\right) \tag{9}$$

where h is the depth of penetration of the apex of the cone beneath the original surface of the indented specimen. In addition, the distribution of the pressure p(r) on the face of the conical indenter is given by

$$p(r) = \left(P/\pi a^2\right) \cosh^{-1}(r/a),\ r \leq a \tag{10}$$

which shows that there is a singularity at r = 0 and that p(r) = 0 at r = a.

Comparison between Meyer's law (Eq. 3) for n = 2 and Sneddon's expression (Eq. 9) shows that if the material behaved elastically, then the constant k becomes equal to 2 E tan α/π $(1 - \nu^2)$ because the diameter of the circle of contact is equal to 2 h tan α for a conical punch. In addition, as the initial portion of the unloading curve of slope dP/dh is often considered to represent elastic response (Fischer-Cripps 2002), application of Eq. 7 allows determination of Young's modulus E,

$$E = P_{max}\pi\left(1 - \nu^2\right)/2 h_e^2 \tan\alpha \tag{11}$$

since $dP/dh = P_{max}/h_e$. However, because the initial portions of the compliance curves obtained for the clay in the present investigation were either vertical or characterized by negative slopes (i.e., increasing penetration with decreasing load), Eq. 11 could not be used to determine values of Young's modulus. As a consequence, the elastic modulus was determined in a different way, as discussed later in the paper.

Remark 3

In indentation testing, pyramidal indenters, like the Vickers pyramid, are generally treated as conical indenters with a cone angle that provides the same area to depth relationship as the actual indenter, despite the availability of contact solutions for pyramidal indenter problems (Fischer-Cripps 2002). This allows the use of axial-symmetric elastic solutions, Eqs. 7 to 10, to be applied to contacts involving non-axial-symmetric indenters. Thus, as the relationship between the projected area of contact A_p and the penetration h_p in Fig. 2 is given by $A_p = 4 h_p^2 \tan^2\theta$ for a Vickers pyramid

with a face angle θ, whereas the relationship is $A_p = \pi h_p^2 \tan^2\alpha$ for a conical indenter, then the Vickers pyramid may be treated as a conical indenter with an effective cone angle given by $\tan^2\alpha = 4 \tan^2\theta/\pi$, resulting, for example, in $\alpha = 69.7^o$ for $\theta = 67.8^o$.

2.3 Rigid-Plastic and Elastic-Plastic Approach

Hill et al. (1947) were the first to examine the plastic flow response of metals indented with different wedge indenters having α varying between 7° and 30°, and concluded that the plastic flow beneath a sharp indenter is cutting in nature. Consequently, Hill (1950) proposed the slip line theory, in which the material beneath the indenter is displaced laterally and upwards from the sides of the wedge. The theory was validated by Dugdale (1953) who performed wedge indentations on cold-worked metals. Atkins and Tabor (1965) systematically studied the indentation response of various metals with conical indenters having α between 30° and 75°, and found that there was a change in plastic flow mechanism from cutting to compressive type at α equal to about 52.5°. It should be also recalled that Shield (1955) obtained a solution for a flat cylindrical punch and Lockett (1963) extended Shield's approach to conical indenters, but was unable to obtain a solution for $\alpha \leq 52.5^o$. Later, Houlsby and Wroth (1982) and Chitkara and Butt (1992) obtained additional solutions. Figure 3 which summarizes the above-mentioned solutions presents values of the so-called cone factor N_c as function of the apical angle 2α for smooth rigid cones. The mean contact pressure at yield p_m is directly related to the undrained shear strength through the factor N_c, that is,

$$p_m = N_c S_u \tag{12}$$

where $S_u = \sigma_y/2$ for Tresca criterion.

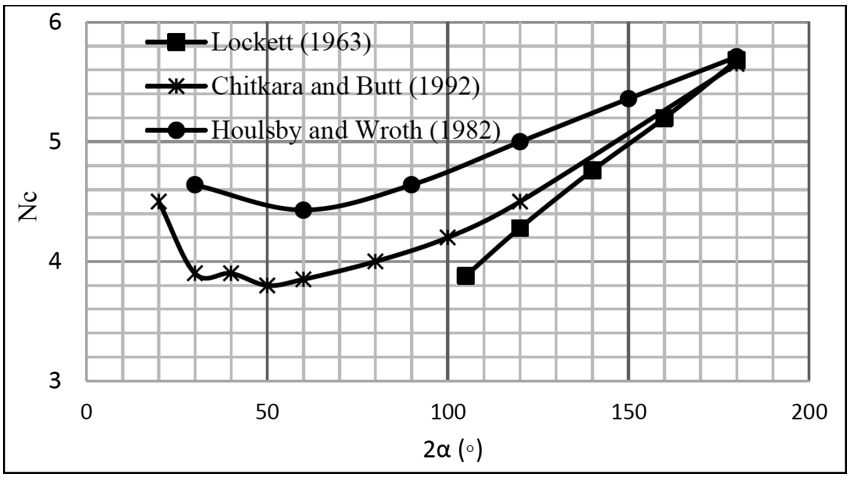

Fig. 3. Cone factor versus apical angle

Samuels and Mulhearn (1957) examined the plastic flow beneath spherical and Vickers indenters and noted that the material under the indenter flowed radially outwards and the elastic-plastic boundary appeared to be hemispherical in shape. These findings were rationalized by recourse to the spherical cavity model of Bishop et al. (1945) and Hill (1950). Later, Mulhearn (1959) conducted indentations experiments on work-hardened steel and concluded that plastic flow occurred via a cutting mechanism under a sharp indenter ($\alpha = 20^{o}$), whereas it was compressive in nature for relatively blunt indenters such as the Vickers pyramid ($\theta = 68^{o}$, $\alpha = 70.3^{o}$).

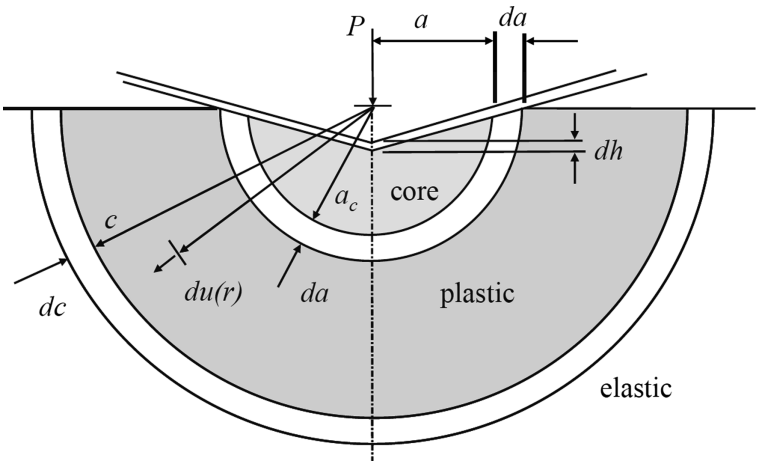

Fig. 4. Expanding cavity model (after Johnson 1970 and Fischer-Cripps 2007)

Dugdale (1954) carried out Vickers indentations on different metals and found that the spherical cavity model could not be used to represent the nature of deformation, because the mean contact pressure needed to expand the cavity was almost twice that required for a shallow penetration. The same observations were made by Marsh (1964) and Hirst and Howse (1969). This led them to suggest that the spherical cavity model had to be modified. On the basis of these results, Johnson (1970) proposed the expanding cavity model or ECM to describe the mean contact pressure for elastic-plastic solids. In this model, the contacting surface of the indenter is encased by a hydrostatic core of radius a_c which in turn is surrounded by a hemispherical plastic core of radius c, as shown in Fig. 4. An increment of penetration dh of the indenter results in an expansion of the core da and the volume displaced by the indenter is accommodated by the radial movement du(r) at the core boundary. This in turn causes the plastic zone to increase in radius by an amount dc. Using this result Johnson (1979) showed that the mean contact pressure p_m for elastic-plastic solids is:

$$p_m = \frac{4}{3}\sigma_y + \frac{2}{3}\sigma_y \ln\left\{\left[E\cot\alpha/\sigma_y + 4(1-2\nu)\right]/6(1-\nu^2)\right\} \qquad (13)$$

and this leads, from Eq. 1, to the following expression for the constraint factor C:

$$C = \frac{4}{3} + \frac{2}{3}\ln\left\{\left[E\cot\alpha\,/\sigma_y + 4\,(1 - 2\nu)\right]/6\,(1 - \nu^2)\right\} \tag{14}$$

Although the ECM constitutes an idealization of the deformation mechanism that takes place beneath a blunt indenter, it nevertheless represents a class of popular models that have the capability to consider the effects of elastic and plastic response on the evolution of the deformation field during indentation (Wang et al. 2016).

In addition, Hainsworth et al. (1996) showed that the loading curve of a specimen could be described using a linear relationship between the load P and the square of the displacement h:

$$P = A^* h^2 \tag{15}$$

Superimposing the displacements arising from both elastic and plastic deformation, the constant of proportionality A* was found to be:

$$A^* = E\{[1/(\pi\tan^2\alpha)]\,[E/H(1 - \nu^2)]^{1/2} + (\pi - 2)\left[H\left(1 - \nu^2\right)/E\right]^{1/2}\}^{-2}/\left(1 - \nu^2\right) \tag{16}$$

This approach provided a good fit to experimental data for specimens with a wide range of modulus and hardness values.

It was also realized in the course of the present study that it is possible to determine the mechanical properties of interest in a "forward" direction rather than in the "reverse" direction, which involves the determination of shape of indentation test results for the deduction of material properties. In the "forward" direction approach, using material parameters (for instance, values of Young's modulus E and yield stress σ_y obtained from unconfined compression tests) as inputs, the expected load-displacement response can be predicted and compared with that obtained experimentally. Alternatively, the expected P vs h^2 relationship for a sharp indenter may be used to determine E and the hardness H by fitting this function to the experimental loading curve. In the present study both approaches were attempted as discussed in the next section.

3 Experimental Investigations

The experimental investigations reported in the present paper were carried out by Ewane (2018). A detailed description of the soil and test procedures may be also found in Ewane et al. (2018).

3.1 Clay

The soil used in this study is an overconsolidated clay of eastern Canada. Undisturbed blocks of clay, 0.3 m in width, were recovered at a depth of 3.5 m in a test excavation. The test site is located 40 km east of Montreal (Quebec), in the town of Beloeil.

The natural water content of the clay varies from 43.7 to 63%, the plastic limit from 20.4 to 33.6%, and the liquid limit from 48.4 to 68%. The clay is overconsolidated, with an overconsolidation ratio (OCR), which is the ratio between the preconsolidation pressure σ_p' and the in situ vertical effective stress σ_{vo}', varying between approximately 5.8 and 8.4. Values of undrained shear strength S_u were determined using miniature vane tests (VST), unconfined compression tests (UU), and Swedish fall-cone tests. Average values of S_u were found to be 33.5 kPa from VSTs, 56.5 kPa from UU tests, and 73.4 kPa from Swedish fall-cone tests. While the lowest value of 33.5 kPa is attributed to the development of cracks around the blades of the miniature vanes upon their insertion, the value of 73.4 kPa obtained from the fall-cone tests is extremely high for such medium overconsolidated clay. As the average preconsolidation pressure σ_p' of the clay is 143.2 kPa, the strength ratio S_u/σ_p' equals 0.233 for the VSTs, 0.396 for the UU tests, and 0.512 for the fall-cone tests. Because measurements have repeatedly shown that the strength ratio for this type of clay falls in the range of 0.25–0.30 (Leroueil et al. 1983), it is believed that the very high value of 0.512 is possibly the result of the very high penetration rate that occurs during the penetration of the falling cone. Typical unconfined compression test results are reported in Fig. 5. Values of Young's modulus E range between 15 and 20 MPa, whereas values of yield stress σ_y vary from 104 to 108 kPa. This figure also shows that the clay may be treated as an elastic perfectly plastic material with a strain-hardening exponent x = 0. Additional UU tests yielded an average value of 113.4 kPa for σ_y which corresponds to $S_u = \sigma_y/2$ (Tresca) or 56.7 kPa.

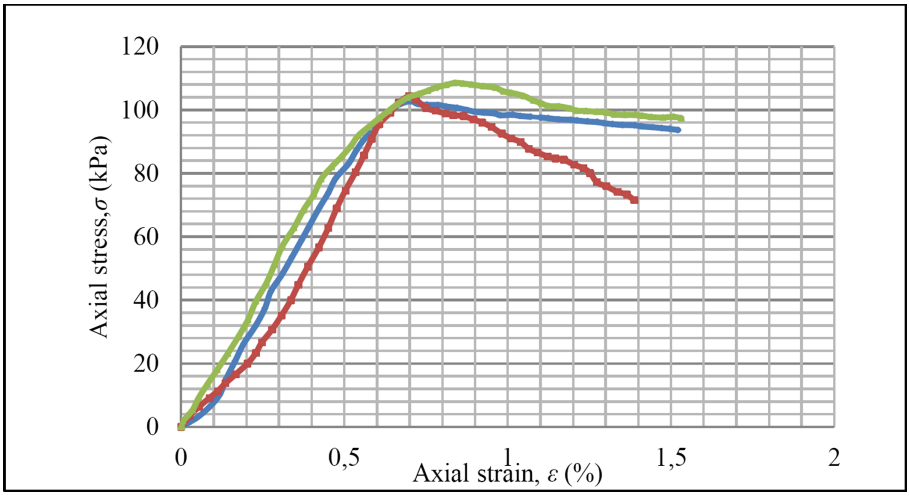

Fig. 5. Unconfined compression test results (after Ewane et al. 2018)

3.2 Indentation Tests

Tests were carried out using a computer-controlled universal testing machine. Indentation tests were performed with 20-mm diameter conical indenters with apical angles 2α of 60^o, 80^o, 97^o, and 144.3^o, as well as with a square-sided Vickers-type pyramid having an equivalent cone apical angle of 139.4^o. The indenters were attached to the top platen of the press and graphite powder was employed to minimize adhesion and friction between the indenters and the clay. The specimens measured 63 mm in diameter and 19 mm in thickness, and were encased in oedometer steel rings for confinement purposes. The specimens which were placed on the bottom platen of the press were raised at a constant rate of 0.5 mm/min. The load and the indenter depth were continuously recorded during each test.

4 Analysis and Discussion of Indentation Test Results

4.1 Determination of Young's Modulus

Typical loading-unloading curves obtained with the indenters are shown in Fig. 6. Although the shapes of the experimental compliance curves are similar at first sight to the general trend illustrated in Fig. 1, the particular form of the initial portions of the unloading branches, which are characterized by either increasing or constant penetration with decreasing load, prevented their use for the determination of the elastic modulus based on Eq. 9 from Sneddon's work. Instead, it was assumed, as suggested by Fischer-Cripps (2002), that the first few experimental points of the loading branches represented a truly elastic response. Thus, the initial portions of the loading branches which are referred to as "Experimental" in Fig. 7 were fitted with expressions of the form $P = k\ h^2$, where $k = 2E \tan \alpha/\pi\ (1 - \nu^2)$ from Eq. 9. Computed values of k and E are reported in Table 1, together with a second set of parameters derived using the same expression, but this time with the fitting applied to the whole loading branches. These are called "Analytical" in Fig. 7. In addition, because $P = k\ h^2$, the mean contact pressure $p_m = P/\pi\ a^2$ or $p_m = k\ h^2/\pi\ a^2 = k \cot \alpha^2/\pi$, where a = radius of circle of contact and $\cot \alpha = h/a$. Values of p_m are also reported in Table 1.

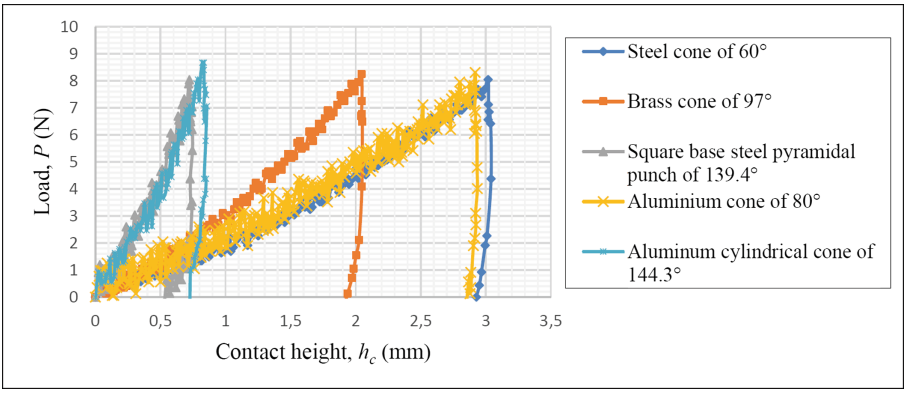

Fig. 6. Experimental compliance curves (after Ewane 2018)

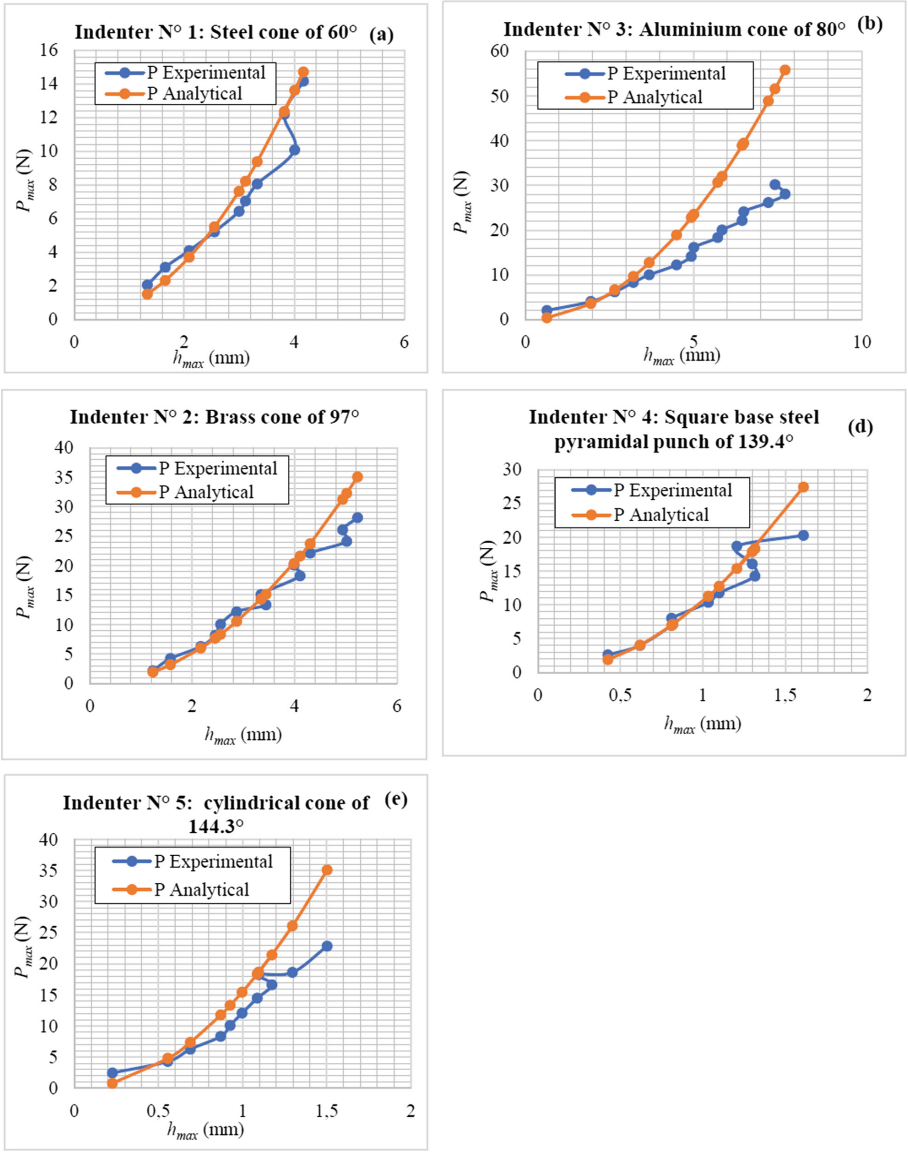

Fig. 7. Fitting of compliance curves (after Ewane 2018)

Examination of the data shown in this table indicates that (a) the computed values of Young's modulus E are much smaller than those deduced from the unconfined compression tests, and (b) the values derived for the sharper cones (i.e., 2α of 60°, 80°, and 97°) are much smaller than those obtained for the blunter ones (i.e., 2α of 139.4° and 144.3°). This shows that the sharper indenters induce more damage to the soil structure than the blunter indenters. As a consequence, realistic values of Young's modulus could not be determined from indentation tests with conical indenters, at least for apical angles $2\alpha \leq 144.3°$.

Table 1. Values of k and E from Sneddon's approach

		Experimental curves			Analytical curves		
Indenter	Apical angle $2\alpha^o$	k (kPa)	E (kPa)	p_m (kPa)	k (kPa)	E (kPa)	p_m (kPa)
Cone	60	615	1254	587	657	1340	627
Cone	80	850	1193	384	940	1320	425
Cone	97	1250	1303	311	1300	1355	384
Pyramid	139.4	10000	4357	436	10657	4650	465
Cone	144.3	12000	4553	396	15560	5903	514

4.2 Determination of Plastic Strength Parameters

For the application of the approach of Hainsworth et al. (1996), it was necessary to determine the hardness H, that is, $H = C\ \sigma_y$. The constraint factor C was computed based upon the results which link C to the ratio $E \cot \alpha/(1 - \nu^2)^2\ \sigma_y$ obtained by Johnson (1970). For E = 17500 kPa, $\nu = 0.5$, and $\sigma_y = 2\ S_u$ =113.4 kPa, the ratio $E \cot \alpha/(1 - \nu^2)\ \sigma_y$ ranges between 66.3 for $2\alpha = 144.3^o$ and 356.4 for $2\alpha = 60^o$. As a result, the constraint factor C = 3 from Johnson (1970)'s data.

The approach proposed by Hainsworth et al. (1996) was considered first for the analysis of indentation test results because it takes into account elastic and plastic response, even though the relationship $P = A^* h^2$ of Eq. 15 has the same form as that derived by Sneddon (1965) for a truly elastic material. Table 2 presents the values of the parameter A* based upon Eq. 16 for E =17500 kPa, $H = 3\sigma_y = 6S_u$ = 340.2 kPa, and $\nu = 0.5$ for undrained conditions from the unconfined compression tests. In this table are also reported the values of the mean contact pressure p_m obtained by assuming that $p_m = A^* \cot^2 \alpha/\pi$, since $p_m = P/\pi\ a^2$. The computed values of A* are compared in Table 2 with the corresponding values of the parameter k determined from the "Analytical" curves of Fig. 7, based upon Sneddon's approach. Examination of the data indicates that although there exists a slightly better agreement for the blunter than for sharper indenters, the values of A* are on average smaller than k. Thus, the approach proposed by Hainsworth et al. (1996) fails to provide an adequate representation of the experimental observations. Comparison between the values of the mean contact pressure p_m reported in Table 2 based upon the "Analytical" curves of Fig. 7 and the hardness $H = 3\sigma_y$ = 340.2 kPa also shows that p_m is on average 42% higher than H.

Values of p_m are compared in Table 3 with those obtained from the analytical curves, as well as from both the approach of Hainsworth et al. (1996) and the expanding cavity model of Johnson (1970). The data show that the computed average value of p_m obtained based on the ECM approach is 16% greater than the value of the hardness H = 340.2 kPa and 22% smaller than the corresponding value (i.e., p_m = 483 kPa) based on the "Analytical" curves of Fig. 7. In addition, the computed values of p_m for the blunter cones of 139.4^o and 144.3^o show good agreement with the value of the hardness H.

Table 2. Comparison between parameters A*, k, and mean contact pressure p_m

		Hainsworth et al. (1996)		Sneddon's approach	
Indenter	Apical angle 2α°	A* (kPa)	p_m (kPa)	k (kPa)	p_m (kPa)
Cone	60	366	350	657	627
Cone	80	732	331	940	425
Cone	97	1316	328	1300	384
Pyramid	139.4	7153	312	10657	465
Cone	144.3	9318	308	15560	514
Average:			326		483

Table 3. Comparison between p_m (kPa) values

Indenter	Apical angle 2α°	Hainsworth et al. (1996)	Sneddon's approach	ECM
Cone	60	350	627	460
Cone	80	331	425	432
Cone	97	328	384	409
Pyramid	139.4	312	465	343
Cone	144.3	308	514	333
Average:		326	483	395

Finally, if the values of the mean contact pressure p_m derived from the "Analytical" curves are considered to correspond to the response of a rigid plastic material, then slip line theory can be applied for the determination of the undrained shear strength S_u. The results which are reported in Table 4 are based on the relationship obtained by Houlsby and Wroth (1982) between the cone factor N_c and the apical angle 2α shown in Fig. 3. In addition, the values of S_u are compared with values deduced from the approaches proposed by Hainsworth et al. (1996) and the expanding cavity model of Johnson (1970). Examination of the different entries in this table shows that the average value of S_u derived from the approach proposed by Hainsworth et al. (1996) agrees well with the value of S_u = 56.7 kPa obtained from the unconfined compression tests. However, such result is caused by the fact that, as the second term in the right-hand side of Eq. 16 is very small compared to the first term, then the parameter A* becomes approximately equal to $H\,\pi\,\tan^2\alpha$. As a consequence, $p_m = H$ because $p_m = A^*\cot^2\alpha$. Thus, $S_u = H/6$ from the approach of Johnson (1970). The data reported in Table 4 also show that whereas the average value of the undrained shear strength obtained from the expanding cavity model is only 16% greater than that found from the unconfined compression tests, the value deduced from application of the slip line theory is unrealistic.

Table 4. Comparison of undrained shear strengths S_u (kPa)

Indenter	Apical angle $2\alpha^o$	Hainsworth et al. (1996)	ECM	Houlsby and Wroth (1982)
Cone	60	58.3	76.7	131.9
Cone	80	55.2	72.0	84.4
Cone	97	54.7	68.2	66.2
Pyramid	139.4	52.0	57.2	83.0
Cone	144.3	51.3	55.5	74.7
Average:		54.3	65.8	88.0

5 Conclusions

The following conclusions are drawn on the basis of the contents of the present study:

1. Realistic values of Young's Realistic values of Young's modulus could not be obtained from the initial portions of the unloading branches of the indentation tests, due to either increasing or constant penetration depth with decreasing load.
2. Application of the elastic solution to the initial portions of the loading branches of the compliance curves showed that the clay suffered severe damage from the beginning of the indentation tests. Such damage which was most severe with the sharp indenters resulted in lower values of Young's modulus.
3. Application of the approaches suggested by Johnson (1970) and Hainsworth et al. (1996) did not allow obtaining a reasonable fitting to the experimental compliance curves. Again, the cause is linked to the severe damage experienced by the clay, especially with the sharper indenters. This notwithstanding, the two approaches permitted the determination of reasonable values for the undrained shear strength.
4. Application of the slip line theory resulted in unreasonable overestimation of the undrained shear strength.
5. Because indentation tests with sharp indenters caused considerable damage to the clay structure, resulting in reduced values of Young' modulus, further investigations should be carried out using either much blunter and spherical indenters, or flat-ended cylindrical punches.

References

American Society for Testing and Materials-ASTM: Standard practice for instrumented indentation testing, E2546-15. ASTM International, pp. 1–24 (2007)

American Society for Testing and Materials-ASTM: Instrumented indentation testing: a Draft ASTM Practice. ASTM International. Standardization News, October 2003

Atkins, A.G., Tabor, D.: Plastic indentation in metals with cones. J. Mech. Phys. Solids **13**(3), 149–164 (1965)

Barquins, M., Maugis, D.: Adhesive contact of axisymmetric punches on an elastic half space: the modified Hertz-Huber's stress tensor for contacting spheres. Journal de Mécanique Théorique et Appliquée **1**(2), 331–357 (1982)

Battacharya, A.K., Nix, W.D.: Finite element simulation of indentation experiments. Int. J. Solids Struct. **24**(12), 141–147 (1988)

Bishop, R.F., Hill, R., Moh, N.F.: The theory of indentation and hardness tests. Proc. Phys. Soc. **57**(3), 147–159 (1945)

Boussinesq, J.: Application des potentiels à l'étude de l'équilibre et du mouvement des solides élastiques: des notes étendues sur divers points de physique mathématique et d'analyse. Gauthier-Villars, Paris, 736 p. (1985)

Cerruti, V.: Ricerche intorno all'equilibrio dei corpi elastici isotropi. Atti Accad. Naz. Lincei Memorie Serie III **XII**, 81–123 (1882)

Cheng, Y.-T., Li, Z.: Hardness obtained from conical indentations with various cone angles. J. Mater. Res. **15**(12), 2830–2855 (2000)

Chitkara, N.R., Butt, M.A.: Numerical construction of axisymmetric slip-line fields for indentation of thick blocks by rigid conical indenters and friction at the tool-metal interface. Int. J. Mech. Sci. **34**(11), 849–862 (1992)

Dugdale, D.S.: Cone indentation experiments. J. Mech. Phys. Solids **2**(4), 265–277 (1954)

Dugdale, D.S.: Wedge indentation experiments with cold-worked metals. J. Mech. Phys. Solids **2** (1), 14–26 (1953)

Ewane, M.-S.: Essais d'indentation sur un sol de la mer Champlain. Ph.D. thesis. École Polytechnique de Montréal, Montréal, Québec, Canada (2018)

Ewane, M.S., Silvestri, V., James, M.: Indentation of a sensitive clay by a flat-ended circular punch. J. Geotech. Geoenviron. Eng. (2018). https://doi.org/10.1007/s10706-018-0561-4

Fischer-Cripps, A.C.: Introduction to Contact Mechanics, 2nd edn. Springer, New York (2007)

Fischer-Cripps, A.C.: Nanoindentation. Springer, New York (2002)

Giannakopoulos, A.E., Larsson, P.L., Vestergaard, R.: Analysis of Vickers indentation. Int. J. Solids Struct. **31**(19), 2679–2708 (1994)

Guha, S., Sangal, S., Basu, S.: Numerical investigations of flat punch molding using a higher order strain gradient plasticity theory. Int. J. Mater. Form. **7**(4), 459–467 (2014)

Hainsworth, S.V., Chandler, H.W., Page, T.F.: Analysis of nanoindentation load displacement loading curves. J. Mater. Res. **11**, 1987–1995 (1996)

Hill, R.: The Mathematical Theory of Plasticity. Oxford University Press, London (1950)

Hill, R., Lee, E.H., Tupper, S.J.: The theory of wedge indentation of ductile materials. Proc. R. Soc. Lond. A **188** (1947). https://doi.org/10.1098/rspa.1947.0009

Hirst, W., Howse, M.G.J.W.: The indentation of materials by wedges. Proc. R. Soc. Lond. A **311** (1969). https://doi.org/10.1098/rspa.1969.0126

Houlsby, G.T., Wroth, C.P.: Direct solution of plasticity problems in soils by the method of characteristics. In: Proceedings of the 4th International Conference on Numerical Methods in Geomechanics, Edmonton, vol. 3, pp. 1059–1071 (1982)

Hu, Z., Lynne, K., Delfanian, F.: Characterization of materials' elasticity and yield strength through micro/nano-indentation testing with a cylindrical flat-tip indenter. J. Mater. Res. **30** (04), 578–591 (2015)

International Organization for Standardization-ISO: Test method for metallic and non-metallic coatings, 14577-4 (2007)

International Organization for Standardization-ISO: Instrumented indentation test for hardness and materials parameters, 14577-1 (2002)

Johnson, K.L.: Contact Mechanics. Cambridge University Press, Cambridge (1985)

Johnson, K.L.: The correlation of indentation experiments. J. Mech. Phys. Solids **18**(2), 115–126 (1970)

Leroueil, S., Tavenas, F., Le Bihan, J.-P.L.: Propriétés caractéristiques des argiles de l'est du Canada. Can. Geotech. J. **20**(4), 681–705 (1983)

Lockett, F.J.: Indentation of a rigid-plastic material by a conical indenter. J. Mech. Phys. Solids **11**(5), 345–355 (1963)
Love, A.E.H.: Boussinesq's problem for a rigid cone. Q. J. Math. **10**(1), 161–175 (1939)
Marsh, D.: Plastic flow in glass. Proc. R. Soc. Lond. A **279**(1378), 420–435 (1964)
Meyer, E.: Untersuchungen über Härteprüfung und Härte Brinell Methoden. Z. Ver. deut. Ing. **52**, 66–74 (1908)
Mulhearn, T.: The deformation of metals by Vickers-type pyramidal indenters. J. Mech. Phys. Solids **7**(2), 85–88 (1959)
Prandtl, L.: Über die Härte plastischer Körper. Nachrichten von der Gesellschaft der Wissenschaften zu Göttingen, Mathematisch-Physikalische Klasse, pp. 74–85 (1920)
Riccardi, B., Montanari, R.: Indentation of metals by a flat-ended cylindrical punch. Mater. Sci. Eng. A **381**, 281–291 (2004)
Samuels, L., Mulhearn, T.: An experimental investigation of the deformed zone associated with indentation hardness impressions. J. Mech. Phys. Solids **5**(2), 125–134 (1957)
Shield, R.T.: On the plastic flow of metals under conditions of axial symmetry. Proc. R. Soc. Lond. A **233**(1193), 267–287 (1955)
Sneddon, I.N.: The relation between load and penetration in the axisymmetric Boussinesq problem for a punch of arbitrary profile. Int. J. Eng. Sci. **3**(1), 47–57 (1965)
Sneddon, I.N.: Boussinesq problem for rigid cone. Math. Proc. **44**(4), 492–507 (1948)
Tabor, D.: The Hardness of Metals. Oxford University Press, London (1951)
Wang, Z., Basu, S., Murthy, T.G., Saldana, C.: Modified expansion theory formulation for circular indentation and experimental validation. Int. J. Solids Struct. **97–98**, 129–136 (2016)
Yu, W., Blanchard, J.P.: An elastic-plastic indentation model and its solutions. J. Mater. Res. **11** (9), 2358–2367 (1996)
Zeng, K., Chiu, C.H.: An analysis of load-penetration curves from instrumented indentation. Acta Mater. **49**(17), 3539–3551 (2001)